Journal of Sound and Vibration (2001) **240**(1), 41–57
doi:10.1006/jsvi.2000.3200, available online at http://www.idealibrary.com on IDEAL®

SYMBOLICAL IMPACT ANALYSIS FOR A FALLING CONICAL ROD AGAINST THE RIGID GROUND

B. Hu, P. Eberhard and W. Schiehlen

Institute B of Mechanics, University of Stuttgart, Pfaffenwaldring 9, *D*-70550 *Stuttgart, Germany*.
E-mail: [*hbi,pe*]*@mechb.uni-stuttgart.de*

(*Received* 14 *March* 2000, *and in final form* 7 *June* 2000)

Longitudinal impact analysis for slender rods has fascinated many famous scientists for hundreds of years. For a rod with uniform cross-sectional area along its length, analytical results about the longitudinal wave propagation of the rod impacting a rigid wall or impacted by a rigid body are well known. However, for a rod with variable cross-sectional area, there exist only a few analytical results in the literature. Since the study of conical rods has recently attracted some interest in various fields, the impact analysis for a conical rod falling against the rigid ground is discussed in this paper in detail and some symbolical results computed by computer algebra are presented. These analytical results are exact and may be used to validate the numerical programs using the finite element method or the boundary element method, too. It is also shown that in contrast to rigid-body collision theory, the geometrical shape of rods plays an important role in impact dynamic.

1. INTRODUCTION

Longitudinal impact analysis has fascinated many famous scientists for hundreds of years and the research results for cylindrical rods or rods with uniform cross-sectional area along their length were reviewed by Goldsmith [1], Graff [2] and Al-Mousawi [3]. In contrast to cylindrical rods, however, only a few investigations were performed for conical rods (see the books by Kolsky [4] and Graff [2]). One reason for this fact is that the wave equations governing conical rods are partial differential equations with variable coefficients due to variable cross-sections of the rods. However, due to the limitation in computing in former times it was not possible to derive analytical solutions, and, e.g., Kolsky's book [4] from 1963 had to stop with the statement of the differential equations for infinitely long rods without wave reflections. Today, people are able to further move the frontier of knowledge using state-of-the-art computer algebra systems and a whole new field of research opens up extending and improving old theories and developing new ones by using these modern computer-aided tools. Recently, it was pointed out that an analysis of conical rods is important, e.g., to the study of foundations, see references [5–7], and to the study of composite structures subjected to high-velocity impact [8]. While we explicitly do not want to focus this paper on these applications (which may be well treatable by FEM), interesting ideas may be found in these areas of research concerning the wave propagation (see, e.g., references [9, 10]). Effects like friction or material damage should not be considered in this paper which is focussed on the wave propagation. In both of the mentioned applications, the dynamic response of a half-plane to a surface load can be determined using a cone model. Hence, vibration of a conical rod was analytically investigated by Abrate [11] and

0022-460X/01/060041 + 17 $35.00/0

Kumar and Sujith [12]. Based on their investigations about the vibration, the wave propagation in a conical rod due to longitudinal impacts is further discussed in this paper.

The wave propagation in a conical rod was to our knowledge first investigated by Landon and Quinney [13]. They studied the problem analytically for an infinite cone of small angle by solving the one-dimensional wave equation for a pulse moving away from the apex. For a finite conical rod where the wave reflection must also be considered, there exist to our knowledge no analytical results for the wave propagation. An experimental investigation for stress wave propagation in a cylindrical bar with a conical end hitting a rigid wall was presented by Suh [14]. For simulation of wave propagation in a cylindrical rod hitting the rigid ground, Shi [15] presented analytical iterated formula where succeeding impacts were also considered. However, the calculation of the supremum in the formula is time-consuming.

In this paper, first the wave equation for a conical rod falling against the rigid ground is described. It is shown that the wave propagation in the conical rod can be described by two one-dimensional functions representing the waves moving forward and backward in the rod. Then, some ordinary differential equations with time delay are derived to determine these two complicated functions, which are then solved with the computer algebra system MAPLE. The reflections of the waves are fully considered and the contact/separation states are treated correctly. Further, a numerical example is used to show the strong influence of the geometrical shape of the rods on the impact behavior. Finally, some conclusions are drawn.

2. MATHEMATICAL MODEL

A conical rod under consideration is homogeneous and linearly elastic. It has Young's modulus E and density ρ. Its length is L and the radius of the cross-section of the conical rod is variable (see Figure 1). The radius at distance x from the lower end of the rod is denoted by $r(x)$ and one can use the abbreviations

$$r_1 = r(0), \quad r_2 = r(L), \quad \alpha = \tan\phi = (r_2 - r_1)/L. \tag{1}$$

Then, the radius of the conical rod at distance x is

$$r(x) = r_1 + \alpha x \tag{2}$$

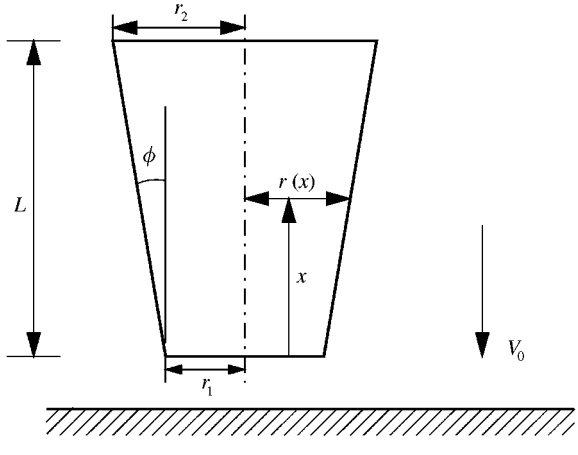

Figure 1. Geometric description of a conical rod.

and the cross-sectional area of the conical rod at distance x is given by

$$A(x) = \pi r^2(x) = \pi(r_1 + \alpha x)^2. \tag{3}$$

The axial displacement and stress in a conical rod at position x and time t are denoted by $u(x, t)$ and $\sigma(x, t)$ respectively. The following relations are used for the velocity:

$$v(x, t) = \dot{u}(x, t) = \frac{\partial u(x, t)}{\partial t} \tag{4}$$

and the strain

$$\varepsilon(x, t) = \frac{\partial u(x, t)}{\partial x}. \tag{5}$$

The material is described by Hooke's law for linear elasticity:

$$\sigma(x, t) = E\varepsilon(x, t). \tag{6}$$

It is assumed that the rod is slender so that its transverse motions can be neglected. The struck ground is rigid and remains at rest during the impact. The contact surface is supposed to be perfectly planar so that St. Venant's contact theory can be used. The resistant force of the air acting on the rod is neglected. According to these assumptions, the governing equation for the longitudinal wave of the rod is an inhomogeneous partial differential equation with varying coefficients,

$$\rho A(x) \frac{\partial^2 u(x, t)}{\partial t^2} = \frac{\partial(A(x)\sigma(x, t))}{\partial x} - \rho A(x) g, \tag{7}$$

where g is the gravitational acceleration. Using equation (3) yields the wave equation for the conical rod,

$$\frac{\partial^2 u(x, t)}{\partial t^2} = c^2 \frac{\partial^2 u(x, t)}{\partial x^2} + \frac{2\alpha c^2}{r(x)} \frac{\partial u(x, t)}{\partial x} - g, \tag{8}$$

where the material parameter $c = \sqrt{E/\rho}$ is the wave propagation velocity. At the beginning of the impact, which is denoted by the time $t = 0$, the rod has uniform velocity along its length and the displacement is zero, i.e.,

$$u(x, 0) = 0, \quad v(x, 0) = -v_0. \tag{9}$$

Since the upper end of the rod is free, the stress at $x = L$ always vanishes and one obtains the boundary condition for the upper end of the rod:

$$\frac{\partial u(L, t)}{\partial x} = 0. \tag{10}$$

For the lower end of the rod, one gets different boundary conditions during the impact and during the free flight. During the impact, the displacement and the velocity at the lower end remain zero:

$$u(0, t) = 0, \quad v(0, t) = 0. \tag{11}$$

On the contrary, during the free flight, the stress at the lower end remains zero,

$$\frac{\partial u(0,t)}{\partial x} = 0. \tag{12}$$

Now the wave equation (8), the initial conditions (9) and the boundary conditions (10) and (11) or (12) are available. Therefore, the mathematical model for the impact problem of a conical rod striking the rigid ground is completely stated.

The wave equation (8) is a non-homogeneous linear partial differential equation with variable coefficients. Multiplying equation (8) by $r(x)$, one can rewrite this equation in the form

$$\frac{\partial^2(r(x)u(x,t))}{\partial t^2} = c^2 \frac{\partial^2(r(x)u(x,t))}{\partial x^2} - gr(x) \tag{13}$$

as shown by Abrate [11]. In order to make all quantities dimensionless, the variables

$$\tau := \frac{ct}{L} \quad \text{and} \quad \xi := \frac{x}{L} \tag{14}$$

are introduced. They denote the dimensionless time and position respectively. Moreover, the dimensionless displacement

$$U(\xi,\tau) := \frac{1}{L} u(x,t) \tag{15}$$

and the dimensionless radius of the rod

$$r^*(\xi) := \frac{1}{L} r(x) = \frac{r_1 + \alpha x}{L} = \frac{r_1}{L} + \alpha\xi \tag{16}$$

are defined. This yields the strain and velocity

$$\frac{\partial u(x,t)}{\partial x} = \frac{\partial U(\xi,\tau)}{\partial \xi} \quad \text{and} \quad \frac{\partial u(x,t)}{\partial t} = c\frac{\partial U(\xi,\tau)}{\partial \tau}. \tag{17}$$

Furthermore, the abbreviation

$$u^*(\xi,\tau) := r^*(\xi)U(\xi,\tau) \tag{18}$$

is introduced. Then, the wave equation (13) turns into

$$\frac{\partial^2 u^*(\xi,\tau)}{\partial \tau^2} = \frac{\partial^2 u^*(\xi,\tau)}{\partial \xi^2} - \beta r^*(\xi), \tag{19}$$

where the constant β is given by

$$\beta := \frac{gL}{c^2}. \tag{20}$$

Differentiating equation (18) with respect to ξ yields

$$\frac{\partial u^*(\xi, \tau)}{\partial \xi} = r^*(\xi) \frac{\partial U(\xi, \tau)}{\partial \xi} + \alpha U(\xi, \tau). \tag{21}$$

From equations (10), (17) and (21), the boundary condition for the upper end of the rod follows:

$$\frac{\partial u^*(1, \tau)}{\partial \xi} = \alpha U(1, \tau) = b u^*(1, \tau) \quad \text{with} \quad b := \frac{\alpha L}{r_2}. \tag{22}$$

Similarly, one can rewrite the boundary condition for the lower end of the rod during the impact as

$$u^*(0, \tau) = 0, \quad \frac{\partial u^*(0, \tau)}{\partial \tau} = 0 \tag{23}$$

and during the free flight as

$$\frac{\partial u^*(0, \tau)}{\partial \xi} = \alpha U(0, \tau) = a u^*(0, \tau) \quad \text{with} \quad a := \frac{\alpha L}{r_1}. \tag{24}$$

Using equation (9) yields the initial conditions for the wave equation (19):

$$u^*(\xi, 0) = 0 \quad \text{and} \quad \frac{\partial u^*(\xi, 0)}{\partial \tau} = -\frac{v_0}{c} r^*(\xi) \quad \text{for } 0 \leqslant \xi \leqslant 1. \tag{25}$$

The new wave equation (19) is still a non-homogeneous linear partial differential equation but now with constant coefficients. According to linear system theory, the solution of the wave equation $u^*(\xi, \tau)$ can be expressed as a sum of a general homogeneous solution $u_g^*(\xi, \tau)$ and a particular solution $u_p^*(\xi, \tau)$,

$$u^*(\xi, \tau) = u_g^*(\xi, \tau) + u_p^*(\xi, \tau). \tag{26}$$

The general homogeneous solution u_g^* satisfies the homogeneous equation

$$\frac{\partial^2 u_g^*(\xi, \tau)}{\partial \tau^2} = \frac{\partial^2 u_g^*(\xi, \tau)}{\partial \xi^2}, \tag{27}$$

and, due to D'Alembert, can be expressed by using two one-dimensional real functions f_1 and f_2:

$$u_g^*(\xi, \tau) = f_1(\tau - \xi) + f_2(\tau + \xi). \tag{28}$$

The function $f_1(\tau - \xi)$ represents the wave moving forward and the function $f_2(\tau + \xi)$ represents the wave moving backward. The particular solution u_p^* can be chosen arbitrarily, however, it must satisfy the wave equation (19). The particular solution

$$u_p^*(\xi, \tau) = -\tfrac{1}{2} \beta r^*(\xi) \tau^2 \tag{29}$$

is chosen. Using equations (26), (28) and (29) yields

$$u^*(\xi, \tau) = f_1(\tau - \xi) + f_2(\tau + \xi) - \tfrac{1}{2} \beta r^*(\xi) \tau^2. \tag{30}$$

Now, the two functions f_1 and f_2 must be determined according to the initial conditions and the boundary conditions of the rod. Differentiating equation (30) with respect to the time τ yields

$$\frac{\partial u^*(\xi, \tau)}{\partial \tau} = f_1'(\tau - \xi) + f_2'(\tau + \xi) - \beta r^*(\xi)\tau, \tag{31}$$

where f_1' and f_2' denote the derivatives of f_1 and f_2 with respect to their arguments. Using the initial conditions (25), i.e., $\tau = 0$, equation (31) yields

$$f_1'(-\xi) + f_2'(\xi) = -\frac{v_0}{c} r^*(\xi) \quad \text{for } 0 \leqslant \xi \leqslant 1. \tag{32}$$

Integrating this equation yields

$$-f_1(-\xi) + f_2(\xi) = -v\left(\alpha_1 \xi + \frac{\alpha}{2}\xi^2\right) + C_1, \tag{33}$$

where the abbreviations v and α_1 denote

$$v = \frac{v_0}{c} \quad \text{and} \quad \alpha_1 = \frac{r_1}{L}. \tag{34}$$

Moreover, from equations (25) and (30) it follows that

$$f_1(-\xi) + f_2(\xi) = 0. \tag{35}$$

From the sum and the difference of equations (33) and (35), one obtains for $0 \leqslant \xi \leqslant 1$

$$f_1(-\xi) = \frac{v}{2}\left(\alpha_1 \xi + \frac{\alpha}{2}\xi^2\right) - \frac{C_1}{2}, \tag{36}$$

$$f_2(\xi) = -\frac{v}{2}\left(\alpha_1 \xi + \frac{\alpha}{2}\xi^2\right) + \frac{C_1}{2}. \tag{37}$$

The constant C_1 can be set to any value since it has no influence on the displacement $u^*(\xi, \tau)$. For simplicity, C_1 can be set to zero. Moreover, for the two one-dimensional functions f_1 and f_2, one can arbitrarily choose their argument variables, for instance, the function $f_1(z) = \sin z$ for $0 \leqslant z \leqslant 1$ and the function $f_1(y) = \sin y$ for $0 \leqslant y \leqslant 1$ are the same function even though they have different arguments z and y; the important point is only the mapping "sinus" for the interval [0, 1]. Since the quantities ξ and τ have a well-defined physical meaning and the arguments of the functions f_1 and f_2 depend on both quantities ξ and τ, a neutral variable y as the argument of the both functions f_1 and f_2 is preferable. Equations (36) and (37) can be rewritten in the form

$$f_1(y) = \frac{v}{2}\left(-\alpha_1 y + \frac{\alpha}{2} y^2\right) \quad \text{for } -1 \leqslant y < 0, \tag{38}$$

$$f_2(y) = -\frac{v}{2}\left(\alpha_1 y + \frac{\alpha}{2} y^2\right) \quad \text{for } 0 \leqslant y < 1. \tag{39}$$

The function $f_1(y)$ is defined now in the interval $-1 \leqslant y \leqslant 0$ and $f_2(y)$ for $0 \leqslant y \leqslant 1$ due to the initial conditions of the rod. Furthermore, these functions in other intervals will be determined also by using the boundary conditions. The boundary condition (22) at the upper end of the rod and equation (30) results in the differential equation

$$-f_1'(\tau - 1) + f_2'(\tau + 1) = b(f_1(\tau - 1) + f_2(\tau + 1)). \tag{40}$$

Upon replacing $(\tau - 1)$ by y in equation (40), an ordinary differential equation with time delay

$$f_2'(y + 2) - f_1'(y) - b(f_2(y + 2) - f_1(y)) = 2bf_1(y) \tag{41}$$

is obtained to determine $f_2(y + 2)$ from $f_1(y)$. If the function f_1 in the interval $[-1, y]$ is known, then the function f_2 in the interval $[1, y + 2]$ can also be computed by solving equation (41). Now the function f_1 needs to be determined. Using the boundary condition (23) at the lower end of the rod during the impact and equation (30) yields

$$f_1(\tau) + f_2(\tau) - \tfrac{1}{2}\,\alpha_1\beta\tau^2 = 0. \tag{42}$$

Replacing τ in equation (42) by y, one obtains

$$f_1(y) = -f_2(y) + \tfrac{1}{2}\,\alpha_1\beta y^2 \tag{43}$$

during the impact. Since the function $f_1(y)$ is already defined in the interval $[-1, 0]$ by equation (38) and $f_2(y)$ in the interval $[0, 1]$ by equation (39), using equation (43), one can compute the function $f_1(y)$ in the interval $(0, 1)$ and using equation (41), one can obtain the function $f_2(y)$ in the succeeding interval $y \in (1, 2)$. Then, using equation (43) once more, one can further calculate the function $f_1(y)$ in the interval $(1, 2)$. Repeating this process, one can get the functions $f_2(y)$ and $f_1(y)$ in the succeeding intervals with length 1 as long as the rod and the ground remain in contact.

One remaining problem now is to determine the duration of contact t_c. Due to equations (5), (6), (7) and (21), the stress is described by the dimensionless time τ and position ξ given by

$$\sigma(\xi, \tau) = E\frac{\partial U(\xi, \tau)}{\partial \xi} = \frac{E}{r^*(\xi)}\left[\frac{\partial u^*(\xi, \tau)}{\partial \xi} - \alpha U(\xi, \tau)\right]. \tag{44}$$

Due to equations (11) and (30), during the impact the stress at the lower end is

$$\sigma(0, \tau) = \frac{E}{r_1}\frac{\partial u^*(0, \tau)}{\partial \xi} = \frac{E}{\alpha_1}\left[-f_1'(\tau) + f_2'(\tau) - \tfrac{1}{2}\,\beta\alpha\tau^2\right]. \tag{45}$$

Using equations (38), (39) and (45), yields for $0 \leqslant \tau < 1$

$$\sigma(0, \tau) = -\frac{E}{\alpha_1}\left[v(\alpha_1 + \alpha\tau) + \alpha_1\beta\tau + \tfrac{1}{2}\,\beta\alpha\tau^2\right] < 0, \tag{46}$$

which means that the duration of contact t_c must be greater then $T := L/c$, i.e., the time taken by a wave to travel once the length of the rod. Therefore, before the wave moving forward is reflected at the upper end of the rod, the lower end of the rod surely remains in contact with the ground. As the stress $\sigma(0, \tau)$ at the lower end of the rod is equal to zero at

the instance $\tau = \tau_c$ and for $\tau > \tau_c$ the stress becomes tensile, the contact ends. The duration of contact corresponding to the dimensionless time τ_c is

$$t_c = \tau_c \frac{L}{c} = \tau_c T. \tag{47}$$

During the free flight, the boundary condition (23) at the lower end of the rod is no longer valid. Instead, the boundary condition (24) should be used. The wave equation (19) and the boundary condition (22) at the upper end of the rod, however, remain true. The displacement $u^*(\xi, \tau)$ still is as given in equation (30) and the function $f_1(y)$ is already available for $-1 \leqslant y \leqslant \tau_c$ and $f_2(y)$ is available for $0 \leqslant y \leqslant \tau_c + 1$, but for $\tau > \tau_c$ equation (43) is no longer valid.

Using equation (30) and the boundary condition (24) at the lower end of the rod yields the differential equation

$$-f_1'(\tau) + f_2'(\tau) = a[f_1(\tau) + f_2(\tau)] \tag{48}$$

during the free flight. During the impact, equation (43) is used to determine the function $f_1(y)$ from $f_2(y)$. During the free flight, equation (48) must be used instead of equation (43). The recursive process for computing the two functions $f_1(y)$ and $f_2(y)$ is similar to the process during the impact.

As the displacement $u(0, t)$ at the lower end of the rod is equal to zero again, the impact begins once more. In the same way, the succeeding impacts and the following motions in the air may be computed.

3. SYMBOLICAL COMPUTATION

The wave propagation in the conical rods resulting from the impact of its lower end hitting the rigid ground can be solved symbolically by using a computer algebra system such as MAPLE [16]. From the above mathematical description of the problem, it can be seen that the main task remaining for the wave propagation analysis is to get the two functions $f_1(y)$ and $f_2(y)$. For their computation, two points should be emphasized. The first point is that due to the impact at the instant $t = 0$ and the succeeding wave reflections, the functions $f_1'(y)$ and $f_2'(y)$ at points $y = 0, 1, 2, \ldots$ are not continuous while the functions $f_1(y)$ and $f_2(y)$ at these points are still continuous. The other point is that the duration of contact is unknown. As the lower end of the rod has different boundary conditions during the impact and during the free flight, the duration of contact τ_c must be determined.

Since the functions $f_1'(y)$ and $f_2'(y)$ at $y = 0, 1, 2, \ldots$ are not continuous, they must be computed piecewisely. The univariant variable y can be decomposed into a couple (n, z) with

$$n = [y] \in \mathbf{N} \quad \text{and} \quad z = y - [y] \in (0, 1), \tag{49}$$

where $[y]$ means the maximal integer not greater than y and $\mathbf{N}$ is the set of all integers. The variable z is the decimal part of y and is always non-negative. The mapping between y and the couple (n, z) is a one-to-one mapping. Then, the functions $f_1(y)$ and $f_2(y)$ can be expressed with the two variables n and z:

$$f_1(y) = f_1^*(n, z) \quad \text{and} \quad f_2(y) = f_2^*(n, z). \tag{50}$$

To determine the functions $f_1^*(n, z)$ and $f_2^*(n, z)$, the recurrence relations for integer $n \in \mathbf{N}$ are needed. Solving the differential equation (41) with the initial condition at $y = n$ yields

$$f_2(y+2) = f_1(y) + [f_2(n+2) - f_1(n)]\,\mathrm{e}^{b(y-n)} + 2b\mathrm{e}^{by}\int_n^y \mathrm{e}^{-by} f_1(y)\,\mathrm{d}y. \tag{51}$$

Using the functions f_1^* and f_2^*, turns it into

$$f_2^*(n+2, z) = f_1^*(n, z) + [f_2^*(n+2, 0) - f_1^*(n, 0)]\mathrm{e}^{bz} + 2b\mathrm{e}^{bz}\int_0^z \mathrm{e}^{-bz} f_1^*(n, z)\,\mathrm{d}z. \tag{52}$$

Due to the continuity of the function $f_2(y)$, it holds true that

$$f_2^*(n+2, 0) = f_2^*(n+1, 1). \tag{53}$$

Therefore, a recurrence relation from the function $f_1^*(n, z)$ and the available quantity $f_2^*(n+1, 1)$ is obtained to determine the next function $f_2^*(n+2, z)$. It yields that

$$f_2^*(n+2, z) = f_1^*(n, z) + [f_2^*(n+1, 1) - f_1^*(n, 0)]\mathrm{e}^{bz} + 2b\mathrm{e}^{bz}\int_0^z \mathrm{e}^{-bz} f_1^*(n, z)\,\mathrm{d}z. \tag{54}$$

During the impact, from equation (43) there follows another recurrence relation to determine $f_1^*(n, z)$ from $f_2^*(n, z)$:

$$f_1^*(n, z) = -f_2^*(n, z) + \tfrac{1}{2}\alpha_1\beta(n+z)^2. \tag{55}$$

Using equations (38) and (39) yields the functions $f_1^*(-1, z)$ and $f_2^*(0, z)$ for the start of the recursion:

$$f_1^*(-1, z) = \frac{v}{2}\left(-\alpha_1(-1+z) + \frac{\alpha}{2}(-1+z)^2\right), \tag{56}$$

$$f_2^*(0, z) = -\frac{v}{2}\left(\alpha_1 z + \frac{\alpha}{2}z^2\right). \tag{57}$$

By means of the start of the recursion relations (56) and (57) and the recurrence relations (54) and (55), all unknown functions $f_1^*(n, z)$ and $f_2^*(n, z)$ during the impact can be determined. Furthermore, it is stated that the functions $f_1^*(n, z)$ and $f_2^*(n, z)$ during the impact can be expressed in a polynomial form

$$f_1^*(n, z) = P_0^{f_1}(n, z) + \mathrm{e}^{bz} P_1^{f_1}(n, z), \tag{58}$$

$$f_2^*(n, z) = P_0^{f_2}(n, z) + \mathrm{e}^{bz} P_1^{f_2}(n, z), \tag{59}$$

where $P_0^{f_1}(n, z)$, $P_1^{f_1}(n, z)$, $P_0^{f_2}(n, z)$ and $P_1^{f_2}(n, z)$ are polynomials of variable z with order depending on the integer n. The reason for this is that the functions $f_1^*(-1, z)$ and $f_2^*(0, z)$ look like

$$P_0^{f_1}(-1, z) = \frac{v}{2}\left[-\alpha_1(-1+z) + \frac{\alpha}{2}(-1+z)^2\right], \quad P_1^{f_1}(-1, z) = 0, \tag{60}$$

$$P_0^{f_2}(0, z) = -\frac{v}{2}\left(\alpha_1 z + \frac{\alpha}{2}z^2\right), \quad P_1^{f_2}(0, z) = 0. \tag{61}$$

The integral $\int_0^z P(z)\,dz$ of a polynomial $P(z)$ is also a polynomial and the integration $\int_0^z e^{-bz}P(z)\,dz$ can be expressed in the form $P_1(z) + e^{-bz}P_2(z)$ where $P_1(z)$ and $P_2(z)$ are two polynomials. Therefore, it can be proved by means of the mathematical induction, and using equations (54) and (55), that the functions $f_1^*(n, z)$ and $f_2^*(n, z)$ have the form given in equations (58) and (59) for all non-negative integers n. Moreover, due to equation (55), the polynomials $P_0^{f_1}(n, z)$ and $P_0^{f_1}(n, z)$ can be computed from the polynomials $P_0^{f_2}(n, z)$ and $P_0^{f_2}(n, z)$:

$$P_0^{f_1}(n, z) = -P_0^{f_2}(n, z) + \frac{1}{2}\alpha\beta(n + z)^2, \tag{62}$$

$$P_1^{f_1}(n, z) = -P_1^{f_2}(n, z). \tag{63}$$

Therefore, during the impact only the polynomials $P_0^{f_2}(n, z)$ and $P_1^{f_2}(n, z)$ are needed. With the help of a computer algebra system, they can be recursively determined for all integers n. For example, some symbolical results for small n are listed here:

$$P_0^{f_2}(1, z) = -\frac{v\alpha_1}{2} + \frac{v\alpha_1 z}{2} - \frac{v\alpha}{4} + \frac{v\alpha z}{2} - \frac{v\alpha z^2}{4} + \frac{v\alpha_1}{b} + \frac{v\alpha}{b} - \frac{v\alpha z}{b} - \frac{v\alpha}{b^2}, \tag{64}$$

$$P_1^{f_2}(1, z) = \frac{v(\alpha_1 b + \alpha b - \alpha)}{b^2}, \tag{65}$$

$$P_0^{f_2}(2, z) = -\frac{v\alpha_1 z}{2} - \frac{v\alpha z^2}{4} - \frac{\alpha_1}{2}\beta z^2 - \frac{v\alpha_1}{b} - \frac{v\alpha z}{b} - \frac{v\alpha}{b^2} - 2\frac{\alpha_1\beta z}{b} - 2\frac{\alpha_1\beta}{b^2}, \tag{66}$$

$$P_1^{f_2}(2, z) = \frac{2v\alpha_1 b - ve^b\alpha_1 b - ve^b\alpha b + ve^b\alpha + 2\alpha_1\beta}{b^2}, \tag{67}$$

$$P_0^{f_2}(3, z) = -\frac{v\alpha_1}{2} - \frac{v\alpha}{4} - \alpha_1\beta z - \frac{\alpha_1\beta}{2} + \frac{v\alpha_1 z}{2} + \frac{v\alpha z}{2} - \frac{v\alpha z^2}{4} - \frac{\alpha_1\beta z^2}{2} - 2\frac{\alpha_1\beta}{b^2} - 2\frac{\alpha_1\beta}{b} + 2\frac{v\alpha_1}{b} - 4\frac{v\alpha}{b^2} - 2\frac{v\alpha z}{b} + 2\frac{v\alpha}{b} - 2\frac{\alpha_1\beta z}{b}, \tag{68}$$

$$P_1^{f_2}(3, z) = \frac{2ve^b\alpha_1 b - 2v\alpha z b - ve^{2b}\alpha_1 b - ve^{2b}\alpha b + ve^{2b}\alpha + 2e^b\alpha_1\beta}{b^2} + \frac{2v\alpha z b^2 - 3v\alpha_1 b - 3v\alpha b + 3v\alpha + 2v\alpha_1 z b^2}{b^2}. \tag{69}$$

However, the duration of contact τ_c must be computed numerically since τ_c is determined by a transcendental function, for which it is impossible to get an analytical solution.

During the free flight, equation (43) is no longer true and equation (48) should be used instead. By using the mapping given in equation (49), the dimensionless duration of contact τ_c is decomposed into an integer n_c and a decimal part z_c as well with

$$n_c = [\tau_c] \quad \text{and} \quad z_c = \tau_c - [\tau_c]. \tag{70}$$

For the function $f_1^*(n_c, z)$ equation (52) remains true only for $z \leqslant z_c$. For $z_c < z < 1$ the boundary condition at the lower end of the rod is changed and another relation must be used. Therefore, two different analytical functions $f_{11}^*(n_c, z)$ for $0 \leqslant z < z_c$ and $f_{12}^*(n_c, z)$ for $z_c \leqslant z < 1$ must be used to describe the function $f_1(n_c, z)$ in the symbolical computation. The piecewise analytical function $f_1^*(n_c, z)$ leads to the fact that after the impact both functions $f_1^*(n, z)$ and $f_2^*(n, z)$ are only piecewise analytic for z in the interval $(0, 1)$. Two different functions $f_{11}^*(n, z)$ and $f_{12}^*(n, z)$ are needed to describe $f_1^*(n, z)$ for $n \geqslant n_c$:

$$f_1^*(n, z) = \begin{cases} f_{11}^*(n, z) & \text{for } 0 \leqslant z < z_c \\ f_{12}^*(n, z) & \text{for } z_c \leqslant z < 1 \end{cases} \tag{71}$$

and two different functions $f_{21}^*(n, z)$ and $f_{22}^*(n, z)$ to describe $f_2^*(n, z)$ for $n \geqslant n_c + 1$

$$f_2^*(n, z) = \begin{cases} f_{21}^*(n, z) & \text{for } 0 \leqslant z < z_c \\ f_{22}^*(n, z) & \text{for } z_c \leqslant z < 1 \end{cases}. \tag{72}$$

For the wave propagation analysis of a conical rod during the free flight after the impact, these four functions $f_{11}^*(n, z)$, $f_{12}^*(n, z)$, $f_{21}^*(n, z)$ and $f_{22}^*(n, z)$ can be recursively determined. Using the boundary condition at the upper end, from equation (54) yields

$$f_{21}^*(n + 2, z) = f_{11}^*(n, z) + [f_{22}^*(n + 1, 1) - f_{11}^*(n, 0)]\mathrm{e}^{bz} + 2b\mathrm{e}^{bz}\int_0^z \mathrm{e}^{-bz} f_{11}^*(n, z)\,\mathrm{d}z, \tag{73}$$

and solving equation (41) with the initial condition at $y = n + z_c$ yields

$$f_2(y + 2) = f_1(y) + [f_2(n + 2 + z_c) - f_1(n + z_c)]\mathrm{e}^{b(y - n - z_c)} + 2b\mathrm{e}^{by}\int_{n + z_c}^{y} \mathrm{e}^{-by} f_1(y)\,\mathrm{d}y, \tag{74}$$

which leads to

$$f_{22}^*(n + 2, z) = f_{12}^*(n, z) + [f_{21}^*(n + 2, z_c) - f_{11}^*(n, z_c)]\mathrm{e}^{b(z - z_c)} + 2b\mathrm{e}^{bz}\int_{z_c}^{z} \mathrm{e}^{-bz} f_{12}^*(n, z)\,\mathrm{d}z. \tag{75}$$

From the boundary condition at the lower end and solving equation (48) with the initial condition at $y = n$, it follows that

$$f_1(y) = f_2(y) + [f_1(n) - f_2(n)]\mathrm{e}^{-a(y - n)} - 2a\mathrm{e}^{-ay}\int_n^y \mathrm{e}^{ay} f_2(y)\,\mathrm{d}y. \tag{76}$$

Similarly, solving equation (48) with the initial condition at $y = n + z_c$ yields

$$f_1(y) = f_2(y) + [f_1(n + z_c) - f_2(n + z_c)]\mathrm{e}^{-a(y-n-z_c)} - 2a\mathrm{e}^{-ay}\int_{n+z_c}^{y} \mathrm{e}^{ay} f_2(y)\,\mathrm{d}y. \tag{77}$$

Due to equations (50), (71) and (72) and the continuity of the functions f_1 and f_2 at $y = n$ and $y = n + z_c$, equations (76) and (77) turn into

$$f_{11}^*(n, z) = f_{21}^*(n, z) + [f_{12}^*(n-1, 1) - f_{22}^*(n-1, 1)]\mathrm{e}^{-az} - 2a\mathrm{e}^{-az}\int_0^z \mathrm{e}^{az} f_{21}^*(n, z)\,\mathrm{d}z, \tag{78}$$

$$f_{12}^*(n, z) = f_{22}^*(n, z) + [f_{11}^*(n, z_c) - f_{21}^*(n, z_c)]\mathrm{e}^{-a(z-z_c)} - 2a\mathrm{e}^{-az}\int_{z_c}^z \mathrm{e}^{az} f_{22}^*(n, z)\,\mathrm{d}z. \tag{79}$$

Now four recurrence relations (73), (75), (78) and (79) to determine four functions $f_{11}^*(n, z)$, $f_{12}^*(n, z)$, $f_{21}^*(n, z)$ and $f_{22}^*(n, z)$ have been obtained. For the start of the recursion, the initial functions

$$f_{11}^*(n_c, z) = f_1^*(n_c, z), \quad f_{12}^*(n_c - 1, z) = f_1^*(n_c - 1, z), \tag{80}$$

$$f_{21}^*(n_c + 1, z) = f_2^*(n_c + 1, z), \quad f_{22}^*(n_c, z) = f_2^*(n_c, z) \tag{81}$$

are used. Therefore, during the free flight, those unknown functions describing the wave propagation can also be recursively determined. The algorithm for the computation of the functions f_1 and f_2 is graphically shown in Figure 2. Furthermore, upon defining a functional set

$$\mathscr{P} := \{f : f = p_0(z) + \mathrm{e}^{bz} p_1(z) + \mathrm{e}^{-az} p_2(z)\} \tag{82}$$

where $p_0(z)$, $p_1(z)$ and $p_2(z)$ are polynomials of z, it can be stated that all functions $f_{11}^*(n, z)$, $f_{12}^*(n, z)$, $f_{21}^*(n, z)$ and $f_{22}^*(n, z)$ are elements of the set $\mathscr{P}$: that is, these functions can be expressed in the analytical form

$$f_{ij}^*(n, z) = P_0^{f_{ij}^*}(n, z) + P_1^{f_{ij}^*}(n, z)\mathrm{e}^{bz} + P_2^{f_{ij}^*}(n, z)\mathrm{e}^{-az} \quad \text{for } i, j = 1, 2, \tag{83}$$

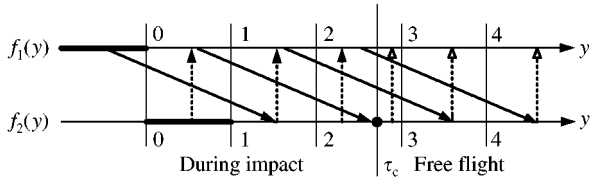

Figure 2. Algorithm for the computation of the functions f_1 and f_2: ——, initial condition; ——→, boundary conditions at the upper end; ---------->, boundary condition at the lower end: during impact; ------->, free flight.

where $P_k^{f_{ij}^*}(n, z)$ for $i, j = 1, 2$ and $k = 0, 1, 2$ are polynomials of z with order depending on n. The reason is that the initial functions $f_{11}^*(n_c, z)$, $f_{12}^*(n_c - 1, z)$, $f_{21}^*(n_c + 1, z)$ and $f_{22}^*(n_c, z)$ are elements of the set and from $f \in \mathscr{P}$

$$e^{-az}\int_0^z e^{az} f \, dz \in \mathscr{P} \quad \text{and} \quad e^{bz}\int_0^z e^{-bz} f \, dz \in \mathscr{P} \tag{84}$$

follows. According to the recurrence relations (73), (75), (78) and (79), it turns out that the functions $f_{11}^*(n, z)$, $f_{12}^*(n, z)$, $f_{21}^*(n, z)$ and $f_{22}^*(n, z)$ have the form as given in equation (83). With these expressions, the symbolical computations can be more efficiently carried out.

4. NUMERICAL EXAMPLES

For conical rods impacting the rigid ground, analytical results for the wave propagation in the rods during the impact can easily be computed symbolically. However, the duration of contact must be computed numerically. For a given duration of contact, analytical results for the wave propagation during the free flight can also be computed symbolically. Since the computer algebra system MAPLE has both symbolical and numerical capabilities, it can be used to deal with the wave propagations in the rods. As an example, three steel rods with the same material $E = 206$ GPa, $\rho = 7900$ kg/m^3, same length $L = 1$ m and same mass are considered. Two conical rods with $\alpha = \pm 0{\cdot}02$ are investigated and compared with a cylindrical rod with $\alpha = 0$ (see Figure 3). The initial impacting velocity v_0 is set to 1 m/s. The duration of contact for the cylindrical rod is $t_c = 2T$, while for the conical rod with $\alpha = 0{\cdot}02$, it is greater ($t_c = 3{\cdot}4T$), and for the conical rod with $\alpha = -0{\cdot}02$, it is smaller ($t_c = 1{\cdot}46T$). Figure 4 shows the contact forces for the three rods. Among the three rods, the

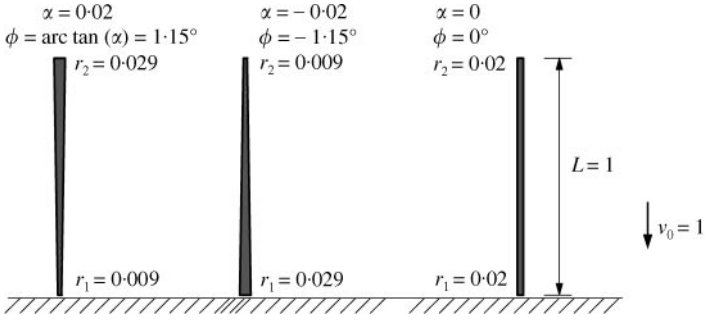

Figure 3. Three different rods for comparison.

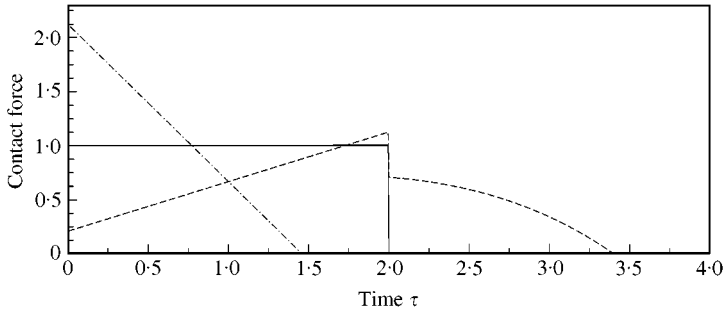

Figure 4. Contact forces $P(t)$ for the three rods: ——, $\alpha = 0$; – – – –, $\alpha = -0{\cdot}02$; –·–·–, $\alpha = 0{\cdot}02$.

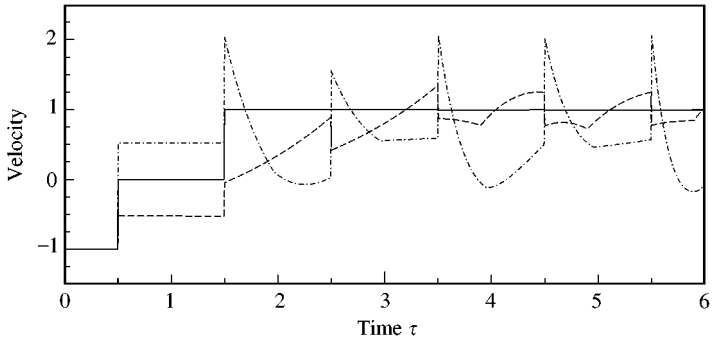

Figure 5. Velocity $v(L/2, t)$ at the center of mass of the rods: ——, $\alpha = 0$; – – –, $\alpha = -0{\cdot}02$; – · – · –, $\alpha = 0{\cdot}02$.

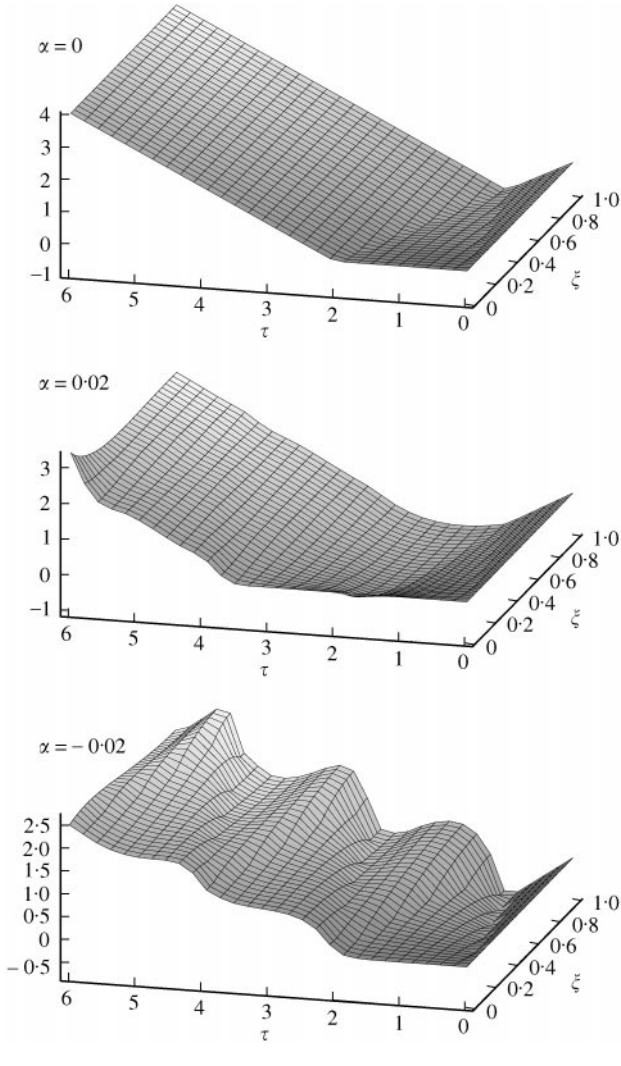

Figure 6. Displacement waves in the three rods.

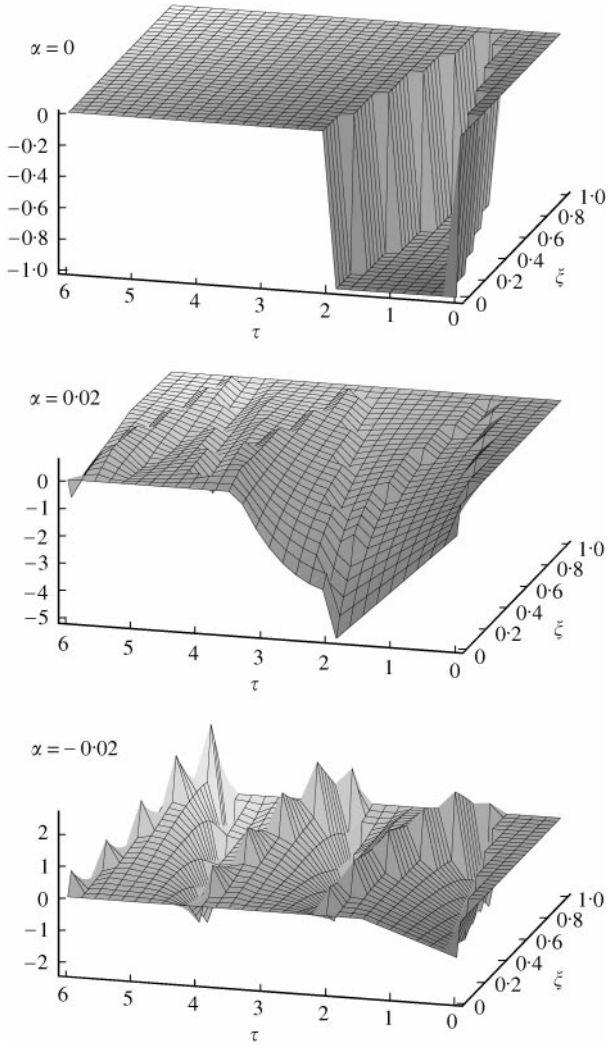

Figure 7. Stress waves in the three rods.

rod with $\alpha = -0{\cdot}02$ has the largest impact force and the shortest duration of contact. Figure 5 shows the velocities at the lower end, in the middle and at the upper end of the rods respectively. It is shown that the conical rod with $\alpha = -0{\cdot}02$ vibrates with the largest amplitude during the free flight. A three-dimensional visualization of the displacement waves and the stress waves in the three rods is shown in Figures 6 and 7 respectively. From these figures, it can be seen that the conical rods have a much more complicated impact behavior than the cylindrical rod.

Often, it is advantageous to use a numerical–symbolical combination to express the responses. For the wave propagation analysis of the conical rods, the most important functions are $f_1^*(n, z)$ and $f_2^*(n, z)$. If numerical values of the system parameters are used, these functions can be recursively determined more easily. For example, the functions $f_1^*(n, z)$ and $f_2^*(n, z)$ for $\alpha = 0{\cdot}02$ are listed in Table 1 in detail so that these results may be used to verify some numerical programs using the finite element method or the boundary element method.

TABLE 1

Numerical-symbolical expressions of $f_1^*(n, z)$ and $f_2^*(n, z)$ for $\alpha = 0{\cdot}02$

$f_1^*(-1, z)$	$1{\cdot}8749 \times 10^{-6} - 2{\cdot}8541 \times 10^{-6} z + 9{\cdot}7915 \times 10^{-7} z^2$
$f_2^*(0, z)$	$-8{\cdot}9578 \times 10^{-7} z - 9{\cdot}7915 \times 10^{-7} z^2$
$f_1^*(0, z)$	$8{\cdot}9578 \times 10^{-6} z + 9{\cdot}8087 \times 10^{-7} z^2$
$f_2^*(1, z)$	$-1{\cdot}8749 \times 10^{-6} - 2{\cdot}8541 \times 10^{-6} z - 9{\cdot}7915 \times 10^{-7} z^2$
$f_1^*(1, z)$	$1{\cdot}8767 \times 10^{-6} + 2{\cdot}8575 \times 10^{-6} z + 9{\cdot}8087 \times 10^{-7} z^2$
$f_2^*(2, z)$	$-1{\cdot}0945 \times 10^{-5} - 6{\cdot}6140 \times 10^{-6} z - 9{\cdot}8087 \times 10^{-6} z^2$ $+ 5{\cdot}2368 \times 10^{-6} e^{0{\cdot}68614z}$
$f_1^*(2, z)$	$1{\cdot}0952 \times 10^{-5} + 6{\cdot}6209 \times 10^{-6} z + 9{\cdot}8259 \times 10^{-6} z^2$ $- 5{\cdot}2368 \times 10^{-6} e^{0{\cdot}68614z}$
$f_2^*(3, z)$	$-1{\cdot}8540 \times 10^{-5} - 8{\cdot}5757 \times 10^{-6} z - 9{\cdot}8087 \times 10^{-7} z^2$ $+ 1{\cdot}0400 \times 10^{-5} e^{0{\cdot}68614z}$
$f_{11}^*(3, z)$	$1{\cdot}8555 \times 10^{-5} + 8{\cdot}5861 \times 10^{-6} z + 9{\cdot}8259 \times 10^{-7} z^2$ $- 1{\cdot}0400 \times 10^{-5} e^{0{\cdot}68614z}$
$f_{12}^*(3, z)$	$1{\cdot}1515 \times 10^{-5} + 6{\cdot}7810 \times 10^{-6} z + 9{\cdot}8087 \times 10^{-7} z^2$ $- 5{\cdot}4314 \times 10^{-6} e^{0{\cdot}68614z} + 2{\cdot}9349 \times 10^{-6} e^{-2{\cdot}1861z}$
$f_{21}^*(4, z) = f_{22}^*(4, z)$	$-3{\cdot}8599 \times 10^{-5} - 1{\cdot}2349 \times 10^{-6} z - 9{\cdot}8259 \times 10^{-7} z^2$ $+ e^{0{\cdot}68614z}(3{\cdot}1158 \times 10^{-5} - 7{\cdot}1863 \times 10^{-6} z)$
$f_{11}^*(4, z) = f_{12}^*(4, z)$	$2{\cdot}8124 \times 10^{-5} + 1{\cdot}0551 \times 10^{-5} z + 9{\cdot}8259 \times 10^{-7} z^2$ $+ e^{0{\cdot}68614z}(-2{\cdot}0080 \times 10^{-5} + 3{\cdot}7529 \times 10^{-6} z) + 7{\cdot}7635 \times 10^{-7} e^{-2{\cdot}1861z}$
$f_{21}^*(5, z)$	$-5{\cdot}1931 \times 10^{-5} - 1{\cdot}4314 \times 10^{-5} z - 9{\cdot}8259 \times 10^{-7} z^2$ $+ e^{0{\cdot}68614z}(4{\cdot}7609 \times 10^{-5} - 1{\cdot}4272 \times 10^{-6} z)$
$f_{22}^*(5, z)$	$-3{\cdot}9615 \times 10^{-5} - 1{\cdot}2499 \times 10^{-5} z - 9{\cdot}8087 \times 10^{-7} z^2$ $+ e^{0{\cdot}68614z}(3{\cdot}4484 \times 10^{-5} - 7{\cdot}4535 \times 10^{-6} z) + 1{\cdot}5327 \times 10^{-6} e^{-2{\cdot}1861z}$
$f_{11}^*(5, z)$	$3{\cdot}9658 \times 10^{-5} + 1{\cdot}2516 \times 10^{-5} z + 9{\cdot}8259 \times 10^{-7} z^2$ $+ e^{0{\cdot}68614z}(-3{\cdot}2427 \times 10^{-5} + 7{\cdot}4535 \times 10^{-6} z) + 8{\cdot}7223 \times 10^{-8} e^{-2{\cdot}1861z}$
$f_{12}^*(5, z)$	$5{\cdot}1974 \times 10^{-5} + 1{\cdot}4431 \times 10^{-5} z + 9{\cdot}8431 \times 10^{-7} z^2$ $+ e^{0{\cdot}68614z}(-4{\cdot}5552 \times 10^{-5} + 1{\cdot}4272 \times 10^{-5} z) + 1{\cdot}6199 \times 10^{-6} e^{-2{\cdot}1861z}$
$f_{21}^*(6, z) = f_{22}^*(6, z)$	$-6{\cdot}7228 \times 10^{-5} - 1{\cdot}6279 \times 10^{-6} z - 9{\cdot}8259 \times 10^{-7} z^2$ $+ e^{0{\cdot}68614z}(6{\cdot}7583 \times 10^{-5} - 2{\cdot}3803 \times 10^{-5} z + 2{\cdot}5750 \times 10^{-6} z^2)$ $+ 4{\cdot}0544 \times 10^{-7} e^{-2{\cdot}1861z}$

5. CONCLUSIONS

In this paper, St. Venant's contact theory has been used to describe the longitudinal wave motion in conical rods. By means of suitable variable transformations, the wave equation for a conical rod may be rewritten into a linear partial equation with constant coefficients. A side effect of these variable transformations is that the boundary conditions become more complicated. By solving this simplified wave equation with the dynamical boundary conditions, analytical results for the wave propagation in conical rods are obtained, where complicated algebraic computations were performed by a computer algebra system. Since the given impact responses are exact and detailed, they may be used to validate numerical programs using finite element methods or boundary element methods. It is shown that among the three compared rods with same mass and same length, the conical rod with larger end impacting the ground has the largest maximum impact force and the shortest duration of contact and vibrates with the largest amplitudes during the free flight, while the conical rod with its smaller end impacting the ground has the largest maximum stress.

REFERENCES

1. W. GOLDSMITH 1960 *Impact*: *The Theory and Physical Behaviour of Colliding Solids*. London: Edward Arnold Ltd.
2. K.F. GRAFF 1975 *Wave Motion in Elastical Solids*. Oxford: Clarendon.
3. M. M. AL-MOUSAWI 1986 *Applied Mechanical Review* **39**, 853–864. On experimental studies of longitudinal and flexural wave propagations: an annotated bibliography.
4. H. KOLSKY 1963 *Stress Waves in Solids*. New York: Dover Publications.
5. J. W. MEEK and J. P. WOLF 1992 *Journal of Geotechnical Engineering* **118**, 667–685. Cone models for homogeneous soil I.
6. J. W. MEEK and J. P. WOLF 1992 *Journal of Geotechnical Engineering* **118**, 686–703. Cone models for rigid rock II.
7. J. W. MEEK and J. P. WOLF 1993 *Earthquake Engineering and Structural Dynamics* **22**, 759–771. Why cone models can represent the elastic half-space.
8. S. ABRATE 1993 *Final Report for Summer Faculty Research Program*, pp. 15.1–15.19, *Air Forces Office of Scientific Research*. Wave propagation during high velocity impacts on composite materials.
9. J. P. WOLF 1994 *Foundation Vibration Analysis using Simple Physical Models*. Englewood Cliffs, NJ: Prentice-Hall.
10. J. P. WOLF and C. SONG 1996 *Finite-Element Modelling of Unbounded Media*. Chichester: Wiley.
11. S. ABRATE 1995 *Journal of Sound and Vibration* **185**, 703–716. Vibration of non-uniform rods and beams.
12. B. M. KUMAR and R. SUJITH 1997 *Journal of Sound and Vibration* **207**, 721–729. Exact solutions for the longitudinal vibration of non-uniform rods.
13. J. W. LANDON and H. QUINNEY 1923 *Proceedings of the Royal Society* **A 103**, 622–643. Experiments with the Hopkinson pressure bar.
14. N. P. SUH 1967 *Experimental Mechanics* **7**, 541–544. Stress-wave propagation in truncated cones against a "rigid" wall.
15. P. SHI 1997 *Computer Methods Applied Mechanics and Engineering* **151**, 497–499. Simulation of impact involving an elastic rod.
16. B. W. CHAR, K. O. GEDDES, G. H. GONNET, M. B. MONAGAN and B. M. WATT 1989 *First Leaves, A Tutorial Introduction to Maple*. Waterloo: Watcom Publications.